Research Article

Advances in Mechanical Engineering

Advances in Mechanical Engineering
2019, Vol. 11(11) 1–13

DOI: 10.1177/1687814019889505
journals.sagepub.com/home/ade
SAGE

Observer-based control for active suspension system with time-varying delay and uncertainty

Kuiyang Wang[1,2], Ren He[1], Heng Li[3], Jinhua Tang[1,2], Ruochen Liu[2], Yangmin Li[4] and Ping He[5,6]

Abstract

Time-varying input delay of actuators, uncertainty of model parameters, and input and output disturbances are important issues in the research on active suspension system of vehicle. In this article, a design methodology involving state observer and observer-based dynamic output-feedback $\mathcal{H}_\infty$ controller considering the above four factors simultaneously is put forward for active suspension system. First, the dynamics equations of active suspension system with time-varying delay are established according to its structure and principle, and its state equations, state observer, and observer-based controller considering time-varying delay, uncertainty of model parameters, and input and output disturbances are given separately. Second, the observer-based controller for quarter-vehicle active suspension system is designed in terms of the linear matrix inequality and the Lyapunov–Krasovskii functional, and the design problem of observer-based controller is converted into the solving problem of linear matrix inequalities. Finally, the gain matrix of observer and the gain matrix of controller are obtained by means of the developed controller and the model parameters of active suspension system; the MATLAB/Simulink model of this system is established; and three numerical simulation cases are given to show the effectiveness of the proposed scheme.

Keywords

Automobile engineering, active suspension system, dynamic output feedback, observer-based controller, time-varying delay, uncertainty, disturbances

Date received: 12 June 2019; accepted: 29 October 2019

Handling Editor: António Mendes Lopes

Introduction

Suspension system, which is located between frame and wheels, mainly consists of spring and shock absorber. It has serious influence on the handling stability and the ride comfort of vehicle and is an important part of vehicle chassis.[1] However, the handling stability and the ride comfort are mutually contradictory. Generally speaking, the good handling stability requires the rigid suspension characteristics, while the good ride comfort requires the soft suspension characteristics. At present, there are three main types of vehicle suspension system: passive suspension system (PSS), semi-active suspension

[1]School of Automotive and Traffic Engineering, Jiangsu University, Zhenjiang, China
[2]School of Automotive and Traffic Engineering, Jiangsu University of Technology, Changzhou, China
[3]Department of Building and Real Estate, The Hong Kong Polytechnic University, Hung Hom, Kowloon, Hong Kong
[4]Department of Industrial and Systems Engineering, The Hong Kong Polytechnic University, Hung Hom, Kowloon, Hong Kong
[5]School of Intelligent Systems Science and Engineering, Jinan University, Zhuhai, China
[6]Department of Automation, Sichuan University of Science & Engineering, Yibin, China

Corresponding author:
Ren He, School of Automotive and Traffic Engineering, Jiangsu University, Zhenjiang 212013, Jiangsu, China.
Email: heren@ujs.edu.cn

Ping He, School of Intelligent Systems Science and Engineering, Jinan University, Zhuhai 519070, Guangdong, China.
Email: pinghecn@qq.com; pinghe@jnu.edu.cn; p.he@polyu.edu.hk

system (SASS) and active suspension system (ASS), in which PSS can't adjust suspension parameters and only be designed in a compromise between the two above performances, and SASS can only adjust the damping of shock absorber according to the driving conditions of vehicle. Compared with PSS and SASS, ASS can automatically adjust the stiffness of spring, the damping of shock absorber, and the height of vehicle body according to the driving conditions of vehicle, and ASS can take into account both of the above properties well synchronously.[2] Therefore, ASS is one of the development directions of vehicle suspension system, and the research on ASS has attracted more and more attention in the recent decades.

ASS is a complex system that integrates machinery,[3] electronics,[4] and hydraulics.[5] Some state variables of ASS are difficult to measure directly, such as acceleration of body vibration, velocity of wheel vibration, and so on, due to the installation location, purchase cost and measurement accuracy of sensors.[6,7] This makes the state feedback control of ASS difficult to realize. The static output-feedback control of ASS is simple and feasible, in which the output variables that can be measured directly are used as the feedback signals. However, the measurable output variables can only reflect the local information of ASS, but not the global information of ASS. Nevertheless, the state observer can reconstruct the state variables of ASS according to the variables which can be measured directly (such as input variables, output variables, etc.), and the reconstructed state variables may be equivalent to the original state variables under the certain indicators.[8] Hence, the observer-based control of ASS is one of the focuses of ASS research. A dynamic output-feedback $\mathcal{H}_\infty$ controller considering input delay was constructed for ASS based on quarter-vehicle model by using linear matrix inequalities (LMIs), and the relatively conservative development conditions were given for multi-objective $\mathcal{H}_\infty$ control[9] of ASS.[10] Aiming at the nonlinearity, unmeasurable state variables, and external disturbances of ASS, a dynamic output-feedback disturbance suppression control strategy was proposed, which was compared with the traditional PID (proportional–integral–derivative) control algorithm to verify the superiority of the proposed design scheme.[11] According to the integration of multiple objectives and LMIs,[12] a $\mathcal{H}_\infty$ control scheme of dynamic output feedback was given for the half vehicle ASS with input delay, the range of allowable input delay was increased, and it was verified by simulation that the good results have been achieved based on suspension performances.[13] In view of the high nonlinearity of the hydraulic actuators in ASS, a high-gain observer was designed to estimate the state variables of ASS based on the suspension displacement which was the only measurable variable, and a development method of $\mathcal{H}_\infty$ controller based on dynamic output feedback for the quarter-vehicle ASS was given based on the proposed high-gain observer and the high-order sliding mode control.[14] An optimal control strategy for ASS with time delay was proposed based on the optimal control theory and the state transform method, and the performances of ASS using the proposed control strategy were analyzed by the vibration experiments of ASS.[15] A preview control method of ASS with time delay was put forward, in which the $\mathcal{H}_\infty$ norm of body acceleration in the finite frequency domain was taken as the optimal performance index and the minimum energy gain in the concerned frequency band was obtained.[16] A control strategy of feedback linearization based on the neural network was proposed for the full vehicle ASS on the basis of particle swarm optimization, and the feasibility of the developed controller was verified through numerical simulation.[17] According to convex optimization and LMIs, a dynamic output-feedback controller with the fixed order considering nonlinear uncertainty was designed for ASS based on quarter-vehicle model, and the model uncertainties, the nonlinear dynamics, and the norm-bounded perturbations were taken into account.[18] Using the second-order sliding mode algorithm, a model-based robust control was given for the fuel cell air-feed system, and the proposed controller was verified to have a good transient performance in the presence of load variations and parametric uncertainties.[19] An output-based adaptive fault-tolerant control method was proposed for nonlinear systems, where the neural network was used to identify the unknown nonlinear characteristics, and an output-based adaptive neural tracking control strategy was developed for the considered system against actuator fault.[20] The safety and reliability of vehicles under delay and uncertainty are important topics; a comprehensive review was given on the fault detection and diagnosis techniques for high-speed trains; and the online fault detection was presented based on the data-driven methods.[21]

Recently, time-varying input delay of actuators,[22] uncertainty of model parameters,[23,24] and input and output disturbances are important issues in the research on the ASS of vehicle. They are interrelated and have important influence on the performances of ASS. However, few of the existing related references involve the above four factors simultaneously, especially the design methodology involving state observer and observer-based controller considering the above four factors simultaneously for ASS based on quarter-vehicle model. The two contributions of this study are summarized simply as follows:

- Based on the Lyapunov–Krasovskii functional and LMIs,[25] a design methodology involving state observer and observer-based dynamic output-feedback $\mathcal{H}_\infty$ controller considering the

above four factors simultaneously is proposed for ASS on the basis of quarter-vehicle model. The state equations, state observer, and observer-based controller of ASS are given separately; the observer-based dynamic output-feedback $\mathcal{H}_\infty$ controller is designed; and the design problem of observer-based controller is converted into the solving problem of LMIs.

- The observer gain matrix and the controller gain matrix are obtained by means of the designed observer-based controller and the technical parameters of selected vehicle; the MATLAB/Simulink model of this system is established; and the numerical simulations of three typical cases are provided to validate the feasibility of the given scheme.

The following sections are arranged as follows. In the "Problem formulation" section, the dynamics equations of ASS with time-varying delay are established according to its structure and principle, and its state equations, state observer, and observer-based controller considering time-varying delay, uncertainty of model parameters, and input and output disturbances are given separately. In the "Main results" section, the observer-based dynamic output-feedback $\mathcal{H}_\infty$ controller for quarter-vehicle ASS is designed in terms of the Lyapunov–Krasovskii functional and LMIs, and the design problem of observer-based controller is converted into the solving problem of LMIs. In the "Numerical simulation" section, the observer gain matrix and the controller gain matrix are obtained by means of the developed controller and the selected model parameters of ASS; the MATLAB/Simulink model of this system is established; and three numerical cases are provided to validate the effectiveness of the designed scheme. In the "Conclusion" section, several conclusions and the following work are given briefly.

Problem formulation

Based on the two degrees of freedom and the quarter-vehicle model, the simplified model of ASS with actuator delay is expressed as Figure 1, where m_s stands for the sprung mass of ASS, m_u indicates the unsprung mass of ASS, $u(t)$ stands for the input signal of ASS, $u(t-h(t))$ indicates the input signal with a actuator delay $h(t)$, c_s and k_s respectively stand for the camping coefficient and the stiffness coefficient of ASS, c_t and k_t denote the camping coefficient and the stiffness coefficient of vehicle tire respectively, and z_s, z_u, and z_r respectively stand for the the moving distance of sprung mass, the moving distance of unsprung mass, and the input displacement of uneven pavement.

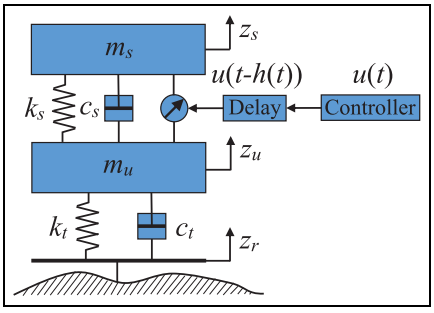

Figure 1. Simplified model of quarter-vehicle ASS.

In the light of the Newton's second law and Figure 1, the dynamics equations of ASS based on quarter-vehicle model are obtained as[26]

$$\begin{cases} \ddot{z}_s(t) = \frac{k_s}{m_s}(z_u(t) - z_s(t)) + \frac{c_s}{m_s}(\dot{z}_u(t) - \dot{z}_s(t)) + \frac{1}{m_s}u(t-h(t)) \\ \ddot{z}_u(t) = \frac{k_s}{m_u}(z_s(t) - z_u(t)) + \frac{c_s}{m_u}(\dot{z}_s(t) - \dot{z}_u(t)) - \frac{1}{m_u}u(t-h(t)) \\ \qquad + \frac{k_t}{m_u}(z_r(t) - z_u(t)) + \frac{c_t}{m_u}(\dot{z}_r(t) - \dot{z}_u(t)) \end{cases} \tag{1}$$

in which $h(t)$ is a known input delay of ASS which satisfies the following inequalities

$$\dot{h}(t) \leqslant \rho_h < 1, 0 \leqslant h(t) \leqslant h^* < \infty \tag{2}$$

where both ρ_h and h^* are positive real numbers.

Based on the actual working characteristics and expectations of ASS, the relative displacement of vehicle body $z_s(t) - z_u(t)$, the relative displacement of vehicle wheel $z_u(t) - z_r(t)$, the velocity of vehicle body vibration $\dot{z}_s(t)$, and the velocity of vehicle wheel vibration $\dot{z}_u(t)$ are selected as the state variables of ASS, that is $x(t) = [z_s(t) - z_u(t), z_u(t) - z_r(t), \dot{z}_s(t), \dot{z}_u(t)]^T \in \mathbb{R}^4$; the velocity of vehicle body vibration $\dot{z}_s(t)$, the relative displacement of vehicle body $z_s(t) - z_u(t)$, and the relative displacement of vehicle wheel $z_u(t) - z_r(t)$ are taken as the control output variables of ASS, that is $z(t) = [\dot{z}_s(t), z_s(t) - z_u(t), z_u(t) - z_r(t)]^T \in \mathbb{R}^3$; the velocity of vehicle body vibration $\dot{z}_s(t)$ and the relative displacement of vehicle body $z_s(t) - z_u(t)$ are chosen as the measurement output variables of ASS, that is $y(t) = [\dot{z}_s(t), z_s(t) - z_u(t)]^T \in \mathbb{R}^2$.

According to equation (1), in consideration of the time-varying delay of actuators, the uncertainty of model parameters, and the input and output disturbances at the same time, the state-space equations of ASS based on quarter-vehicle model may be obtained as follows

$$\begin{cases} \dot{x}(t) = (A + \Delta A)x(t) + (B + \Delta B)u(t - h(t)) + W_1 w_1(t) \\ z(t) = C_1 x(t) \\ y(t) = C_2 x(t) + W_2 w_2(t) \end{cases} \tag{3}$$

in which $w_1(t) = \dot{z}_r(t)$ shows the input disturbance of ASS which is caused by uneven pavement, $w_2(t)$ shows the output disturbance of ASS which is caused by sensor measurement, and

$$A = \begin{bmatrix} 0 & 0 & 1 & -1 \\ 0 & 0 & 0 & 1 \\ \frac{-k_s}{m_s} & 0 & \frac{-c_s}{m_s} & \frac{c_s}{m_s} \\ \frac{k_s}{m_u} & \frac{-k_t}{m_u} & \frac{c_s}{m_u} & \frac{-c_s-c_t}{m_u} \end{bmatrix}, B = \begin{bmatrix} 0 \\ 0 \\ \frac{1}{m_s} \\ -\frac{1}{m_u} \end{bmatrix},$$

$$W_1 = \begin{bmatrix} 0 \\ -1 \\ 0 \\ \frac{c_t}{m_u} \end{bmatrix}, C_1 = \begin{bmatrix} 0 & 0 & 1 & 0 \\ 1 & 0 & 0 & 0 \\ 0 & 1 & 0 & 0 \end{bmatrix},$$

$$C_2 = \begin{bmatrix} 0 & 0 & 1 & 0 \\ 1 & 0 & 0 & 0 \end{bmatrix}, W_2 = \begin{bmatrix} \alpha_1 \\ \alpha_2 \end{bmatrix}$$

in which both α_1 and α_2 are the weight coefficients of sensor disturbance.

Suppose both of ΔA and ΔB are the matrices of uncertain parameters which are norm-bounded, so the uncertainty of ASS parameters may be expressed as

$$[\Delta A, \Delta B] = HF(t)[E_1, E_2] \tag{4}$$

in which $F(t)$ indicates a matrix which is time-varying and meets $F^T(t)F(t) \leqslant I$, in which I indicates a unit matrix; H, E_1, and E_2 are the matrices with known real constants.

According to the state-space equations of quarter-vehicle ASS (equation (3)), the state observer and the observer-based controller of ASS may be expressed as below

$$\begin{cases} \dot{\hat{x}}(t) = A\hat{x}(t) + Bu(t) + L[y(t) - \hat{y}(t)] \\ \hat{y}(t) = C_2\hat{x}(t) \end{cases} \tag{5}$$

and

$$u(t) = K\hat{x}(t) \tag{6}$$

in which $\hat{x}(t) \in \mathbb{R}^4$ expresses the observer-based state vector of ASS, L expresses the gain matrix of proposed observer, and K expresses the gain matrix of observer-based controller.

Main results

The state observer and the observer-based controller considering the above four factors simultaneously will be constructed for ASS based on quarter-vehicle model using the Lyapunov–Krasovskii functional and LMIs in this section, and the design of observer-based controller will be converted into the solving problem of LMIs.

Theorem 1. For the quarter-vehicle ASS (equation (3)), if there are symmetric positive-definite matrices $P_1, P_2 \in \mathbb{R}^{n\times n}$, and given scalar $\gamma > 1$, the following *LMIs* hold

$$\begin{bmatrix} P_1A + A^TP_1 + 2E_1^TE_1 + C_1^TC_1 + U_1 & P_1W_1 & 0 & P_1 \\ \star & (1-\gamma^2)I & 0 & 0 \\ \star & \star & (1-\gamma^2)I & 0 \\ \star & \star & \star & -U_2^{-1} \end{bmatrix} < 0 \tag{7}$$

$$\begin{bmatrix} P_2A + A^TP_2 - 2C_2^TC_2 + C_2^TW_2W_2^TC_2 & P_2 \\ \star & -V^{-1} \end{bmatrix} < 0 \tag{8}$$

where "$\star$" denotes the matrix obtained by matrix symmetry, and

$$U_1 = P_2\left[\left(1 + \frac{2}{1-\rho_h}\right)BB^T + \frac{2}{1-\rho_h}BE_2^TE_2B^T\right]P_2$$
$$U_2 = 3HH^T + 2BB^T$$
$$V = 3HH^T + \left(5 + \frac{2}{1-\rho_h}\right)BB^T + \frac{2}{1-\rho_h}BE_2^TE_2B^T + W_1W_1^T$$

then the quarter-vehicle ASS (equation (3)) with the state observer (equation (5)) and the observer-based controller (equation (6)) where

$$K = B^TP_2, L = P_2^{-1}C_2^T \tag{9}$$

is asymptotically stable. ■

Proof. Let the error of state observer $e(t) \triangleq x(t) - \hat{x}(t)$; according to equations (3), (5), and (6), $\dot{x}(t)$ and $\dot{\hat{x}}(t)$ may be expressed as follows, respectively

$$\dot{x}(t) = (A + \Delta A)x(t) + (B + \Delta B)Kx(t - h(t)) - (B + \Delta B)Ke(t - h(t)) + W_1w_1(t) \tag{10}$$

$$\dot{\hat{x}}(t) = (A + BK)x(t) - (A + BK - LC_2)e(t) + LW_2w_2(t) \tag{11}$$

From equations (10) and (11), $\dot{e}(t)$ may be expressed as

$$\begin{aligned} \dot{e}(t) &= \dot{x}(t) - \dot{\hat{x}}(t) \\ &= (\Delta A - BK)x(t) + (A + BK - LC_2)e(t) \\ &+ (B + \Delta B)Kx(t - h(t)) \\ &-(B + \Delta B)Ke(t - h(t)) + W_1w_1(t) - LW_2w_2(t) \end{aligned} \tag{12}$$

From equations (10) and (12), the augmented system may be given as follows

$$\begin{bmatrix}\dot{x}(t)\\ \dot{e}(t)\end{bmatrix} = \begin{bmatrix} A+\Delta A & 0 \\ \Delta A - BK & A+BK-LC_2\end{bmatrix} \begin{bmatrix}x(t)\\ e(t)\end{bmatrix} + \begin{bmatrix}(B+\Delta B)K & -(B+\Delta B)K \\ (B+\Delta B)K & -(B+\Delta B)K\end{bmatrix}\begin{bmatrix}x(t-h(t))\\ e(t-h(t))\end{bmatrix} + \begin{bmatrix}W_1 & 0\\ W_1 & -LW_2\end{bmatrix}\begin{bmatrix}w_1(t)\\ w_2(t)\end{bmatrix} \tag{13}$$

Introduce the Lyapunov–Krasovskii functional as below

$$V(x(t),e(t)) = \begin{bmatrix}x^T(t) & e^T(t)\end{bmatrix}\begin{bmatrix}P_1 & 0\\ 0 & P_2\end{bmatrix}\begin{bmatrix}x(t)\\ e(t)\end{bmatrix} + \int_{t-h(t)}^{t}\begin{bmatrix}x^T(s) & e^T(s)\end{bmatrix}\begin{bmatrix}R_1 & 0\\ 0 & R_2\end{bmatrix}\begin{bmatrix}x(s)\\ e(s)\end{bmatrix}ds \tag{14}$$

in which P_1, P_2, R_1, and R_2 are the matrices which are symmetric positive-definite.

From equations (2) and (14), $\dot{V}(x(t),e(t))$ may be expressed as

$$\begin{aligned}\dot{V}(x(t),e(t)) &= 2\begin{bmatrix}x^T(t) & e^T(t)\end{bmatrix}\begin{bmatrix}P_1 & 0\\ 0 & P_2\end{bmatrix}\begin{bmatrix}\dot{x}(t)\\ \dot{e}(t)\end{bmatrix} \\ &+ x^T(t)R_1x(t) + e^T(t)R_2e(t) \\ &-\big(1-\dot{h}(t)\big)x^T(t-h(t))R_1x(t-h(t)) \\ &-\big(1-\dot{h}(t)\big)e^T(t-h(t))R_2e(t-h(t)) \\ &\leqslant 2\begin{bmatrix}x^T(t) & e^T(t)\end{bmatrix}\begin{bmatrix}P_1 & 0\\ 0 & P_2\end{bmatrix}\begin{bmatrix}\dot{x}(t)\\ \dot{e}(t)\end{bmatrix} \\ &+ x^T(t)R_1x(t) + e^T(t)R_2e(t) \\ &-(1-\rho_h)x^T(t-h(t))R_1x(t-h(t)) \\ &-(1-\rho_h)e^T(t-h(t))R_2e(t-h(t))\end{aligned} \tag{15}$$

Assuming that there are no input and output disturbances, that is $w_1(t) = w_2(t) = 0$, then equation (15) may be represented as follows in the light of equation (13)

$$\begin{aligned}&\dot{V}(x(t),e(t)) \leqslant 2x^T(t)P_1(A+\Delta A)x(t) + 2e^T(t) \\ &P_2(\Delta A - BK)x(t) + 2e^T(t)P_2(A+BK-LC_2)e(t) \\ &+ 2x^T(t)P_1(B+\Delta B)Kx(t-h(t)) - 2x^T(t)P_1(B+\Delta B)Ke(t-h(t)) \\ &+ 2e^T(t)P_2(B+\Delta B)Kx(t-h(t)) - 2e^T(t)P_2(B+\Delta B)Ke(t-h(t)) \\ &+ x^T(t)R_1x(t) + e^T(t)R_2e(t) - (1-\rho_h)x^T(t-h(t))R_1x(t-h(t)) \\ &- (1-\rho_h)e^T(t-h(t))R_2e(t-h(t))\end{aligned} \tag{16}$$

From Lemma 1 in Appendix 1, we are able to get the following inequalities

$$-2e^T(t)P_2BKx(t) \leqslant x^T(t)K^TKx(t) + e^T(t)P_2BB^TP_2e(t) \tag{17}$$

$$\begin{aligned}&2x^T(t)P_1BKx(t-h(t)) \leqslant x^T(t)P_1BB^TP_1x(t) \\ &+ x^T(t-h(t))K^TKx(t-h(t))\end{aligned} \tag{18}$$

$$\begin{aligned}&-2x^T(t)P_1BKe(t-h(t)) \leqslant x^T(t)P_1BB^TP_1x(t) \\ &+ e^T(t-h(t))K^TKe(t-h(t))\end{aligned} \tag{19}$$

$$\begin{aligned}&2e^T(t)P_2BKx(t-h(t)) \leqslant e^T(t)P_2BB^TP_2e(t) \\ &+ x^T(t-h(t))K^TKx(t-h(t))\end{aligned} \tag{20}$$

$$\begin{aligned}&-2e^T(t)P_2BKe(t-h(t)) \leqslant e^T(t)P_2BB^TP_2e(t) \\ &+ e^T(t-h(t))K^TKe(t-h(t))\end{aligned} \tag{21}$$

From equation (4) and Lemma 2 in Appendix 1, we are able to get the inequalities as below

$$2x^T(t)P_1\Delta Ax(t) \leqslant x^T(t)E_1^TE_1x(t) + x^T(t)P_1HH^TP_1x(t) \tag{22}$$

$$2e^T(t)P_2\Delta Ax(t) \leqslant x^T(t)E_1^TE_1x(t) + e^T(t)P_2HH^TP_2e(t) \tag{23}$$

$$\begin{aligned}&2x^T(t)P_1\Delta BKx(t-h(t)) \leqslant x^T(t)P_1HH^TP_1x(t) \\ &+ x^T(t-h(t))K^TE_2^TE_2Kx(t-h(t))\end{aligned} \tag{24}$$

$$\begin{aligned}&-2x^T(t)P_1\Delta BKe(t-h(t)) \leqslant x^T(t)P_1HH^TP_1x(t) \\ &+ e^T(t-h(t))K^TE_2^TE_2Ke(t-h(t))\end{aligned} \tag{25}$$

$$\begin{aligned}&2e^T(t)P_2\Delta BKx(t-h(t)) \leqslant e^T(t)P_2HH^TP_2e(t) \\ &+ x^T(t-h(t))K^TE_2^TE_2Kx(t-h(t))\end{aligned} \tag{26}$$

$$\begin{aligned}&-2e^T(t)P_2\Delta BKe(t-h(t)) \leqslant e^T(t)P_2HH^TP_2e(t) \\ &+ e^T(t-h(t))K^TE_2^TE_2Ke(t-h(t))\end{aligned} \tag{27}$$

From equations (17)–(27), equation (16) may be shown as below

$$\begin{aligned}&\dot{V}(x(t),e(t)) \leqslant x^T(t)Q_1x(t) + e^T(t)Q_2e(t) \\ &+ x^T(t-h(t))\big[2K^TK + 2K^TE_2^TE_2K - (1-\rho_h)R_1\big]x(t-h(t)) \\ &+ e^T(t-h(t))\big[2K^TK + 2K^TE_2^TE_2K - (1-\rho_h)R_2\big]e(t-h(t))\end{aligned} \tag{28}$$

where

$$\begin{aligned}Q_1 &= P_1A + A^TP_1 + 2E_1^TE_1 + 3P_1HH^TP_1 \\ &+ 2P_1BB^TP_1 + K^TK + R_1, \\ Q_2 &= P_2A + A^TP_2 + P_2BK + K^TB^TP_2 \\ &- P_2LC_2 - C_2^TL^TP_2 + 3P_2BB^TP_2 + 3P_2HH^TP_2 + R_2\end{aligned}$$

In order to simplify equation (28), we set $R_1 = R_2 = (2/(1-\rho_h))(K^TK + K^TE_2^TE_2K)$; then equation (28) becomes

$$\dot{V}(x(t),e(t)) \leqslant x^T(t)Q_1x(t) + e^T(t)Q_2e(t) \tag{29}$$

Simultaneously, Q_1 and Q_2 can be changed as follows from equation (9)

$$Q_1 = P_1A + A^TP_1 + 2E_1^TE_1 + P_1\left(3HH^T + 2BB^T\right)P_1 + P_2\left(BB^T + \frac{2}{1-\rho_h}BB^T + \frac{2}{1-\rho_h}BE_2^TE_2B^T\right)P_2 \tag{30}$$

$$Q_2 = P_2A + A^TP_2 - 2C_2^TC_2 + P_2\left(3HH^T + 5BB^T + \frac{2}{1-\rho_h}BB^T + \frac{2}{1-\rho_h}BE_2^TE_2B^T\right)P_2 \tag{31}$$

For the active suspension system (equation (3)), $\mathcal{H}_\infty$ performance index is taken as follows

$$J_T = \int_0^T \left[z^T(t)z(t) - \gamma^2 w_1^T(t)w_1(t) - \gamma^2 w_2^T(t)w_2(t)\right]dt \tag{32}$$

Considering $T>0$ and any nonzero perturbations, in the light of equation (14) with zero initial conditions, equation (32) may be converted to

$$\begin{aligned} J_T &= \int_0^T \left[z^T(t)z(t) - \gamma^2 w_1^T(t)w_1(t) - \gamma^2 w_2^T(t)w_2(t) + \dot{V}(x(t),e(t)) - \dot{V}(x(t),e(t))\right]dt \\ &= \int_0^T \left[z^T(t)z(t) - \gamma^2 w_1^T(t)w_1(t) - \gamma^2 w_2^T(t)w_2(t) + \dot{V}(x(t),e(t))\right]dt - S_1 - S_2 \end{aligned} \tag{33}$$

where

$$S_1 = \begin{bmatrix} x^T(T) & e^T(T)\end{bmatrix}\begin{bmatrix} P_1 & 0 \\ 0 & P_2\end{bmatrix}\begin{bmatrix} x(T) \\ e(T)\end{bmatrix},$$

$$S_2 = \int_{T-h(T)}^{T} \begin{bmatrix} x^T(s) & e^T(s)\end{bmatrix}\begin{bmatrix} R_1 & 0 \\ 0 & R_2\end{bmatrix}\begin{bmatrix} x(s) \\ e(s)\end{bmatrix}ds$$

Obviously, $S_1 \geqslant 0$ and $S_2 \geqslant 0$. Then equation (33) becomes

$$J_T \leqslant \int_0^T \left[z^T(t)z(t) - \gamma^2 w_1^T(t)w_1(t) - \gamma^2 w_2^T(t)w_2(t) + \dot{V}(x(t),e(t))\right]dt \tag{34}$$

From equations (3), (13), (15), and (29), equation (34) may be shown as below

$$\begin{aligned} J_T \leqslant \int_0^T &\left[x^T(t)C_1^TC_1x(t) - \gamma^2 w_1^T(t)w_1(t) - \gamma^2 w_2^T(t)w_2(t) + x^T(t)Q_1x(t).\right. \\ &+ e^T(t)Q_2e(t) + 2x^T(t)P_1W_1w_1(t) + 2e^T(t) \\ &\left.P_2W_1w_1(t) - 2e^T(t)P_2LW_2w_2(t)\right]dt \end{aligned} \tag{35}$$

From Lemma 1 in Appendix 1, we are able to get the following inequalities

$$2e^T(t)P_2W_1w_1(t) \leqslant e^T(t)P_2W_1W_1^TP_2e(t) + w_1^T(t)w_1(t) \tag{36}$$

$$-2e^T(t)P_2LW_2w_2(t) \leqslant e^T(t)P_2LW_2W_2^TL^TP_2e(t) + w_2^T(t)w_2(t) \tag{37}$$

According to equations (36) and (37), equation (35) can be converted to

$$J_T \leqslant \int_0^T \begin{bmatrix} x(t) \\ w_1(t) \\ w_2(t)\end{bmatrix}^T M_1 \begin{bmatrix} x(t) \\ w_1(t) \\ w_2(t)\end{bmatrix}dt + \int_0^T e^T(t)M_2e(t)dt \tag{38}$$

where

$$M_1 = \begin{bmatrix} Q_1 + C_1^TC_1 & P_1W_1 & 0 \\ \star & (1-\gamma^2)I & 0 \\ \star & \star & (1-\gamma^2)I\end{bmatrix},$$

$$M_2 = Q_2 + P_2W_1W_1^TP_2 + P_2LW_2W_2^TL^TP_2$$

According to equation (30) and the Schur complement theorem (Lemma 3 in Appendix 1), $M_1<0$ is equivalent to

$$\begin{bmatrix} P_1A + A^TP_1 + 2E_1^TE_1 + C_1^TC_1 + U_1 & P_1W_1 & 0 & P_1 \\ \star & (1-\gamma^2)I & 0 & 0 \\ \star & \star & (1-\gamma^2)I & 0 \\ \star & \star & \star & -U_2^{-1}\end{bmatrix} < 0 \tag{39}$$

where

$$U_1 = P_2\left[\left(1 + \left(\frac{2}{(1-\rho_h)}\right)\right)BB^T + \frac{2}{1-\rho_h}BE_2^TE_2B^T\right]P_2,$$

$$U_2 = 3HH^T + 2BB^T$$

From equation (9), equation (31), and the Schur complement theorem (Lemma 3 in Appendix 1), $M_2<0$ is equivalent to

$$\begin{bmatrix} P_2A + A^TP_2 - 2C_2^TC_2 + C_2^TW_2W_2^TC_2 & P_2 \\ \star & -V^{-1}\end{bmatrix} < 0 \tag{40}$$

where

$$V = 3HH^T + \left(5 + \left(\frac{2}{(1-\rho_h)}\right)\right)BB^T + \frac{2}{1-\rho_h}BE_2^TE_2B^T + W_1W_1^T$$

From equations (7) and (8), it's easy to find $M_1 < 0$ and $M_2 < 0$.

It is obvious from equation (38): $J_T < 0$, and equation (32) can be expressed as follows with T tending to infinity

$$\int_0^{+\infty} z^T(t)z(t)dt < \gamma^2 \int_0^{+\infty} \left[w_1^T(t)w_1(t) + w_2^T(t)w_2(t)\right]dt \tag{41}$$

Hence, the quarter-vehicle ASS (equation (3)) with the proposed observer (equation (5)) and the developed controller (equation (6)), where $K = B^TP_2$ and $L = P_2^{-1}C_2^T$, is asymptotically stable. The proof is completed. □

Numerical simulation

The simulation results of several numerical cases are given to verify the correctness and practicability of the proposed scheme. The related parameters of ASS model are listed as follows: $m_u = 114$ kg, $m_s = 973$ kg, $c_t = 14.6$ Ns/m, $c_s = 1095$ Ns/m, $k_t = 101,115$ N/m, and $k_s = 42,720$ N/m.[10] Based on equations (3), (5), and (6), the block diagram of quarter-vehicle ASS with input delay of actuators, uncertainty of model parameters, and input and output disturbances is given as Figure 2.

The numerical simulation model of the ASS mentioned above based on a quarter-vehicle model is set up as Figure 3, based on MATLAB/Simulink software.

In view of equation (2), the input delay of ASS actuator is set as $h(t) = -\exp(-(t + 1/100)) \times \sin(t) \times (\cos(t))^2 + 1$, so the signal curves of $h(t)$ and $\dot{h}(t)$ may be expressed as Figure 4.

On the basis of the LMIs (equations (7) and (8)), K and L may be obtained as follows

$$K = [668.9 \quad 1961.1 \quad 368.8 \quad -325.6],$$

$$L = \begin{bmatrix} -0.6932 & 0.2499 \\ -0.1212 & 0.0260 \\ 8.6685 & -0.6932 \\ 1.2336 & -0.4285 \end{bmatrix}$$

In accordance with equation (4), the time-varying matrices of uncertainty parameters with norm-bounded are respectively taken as follows

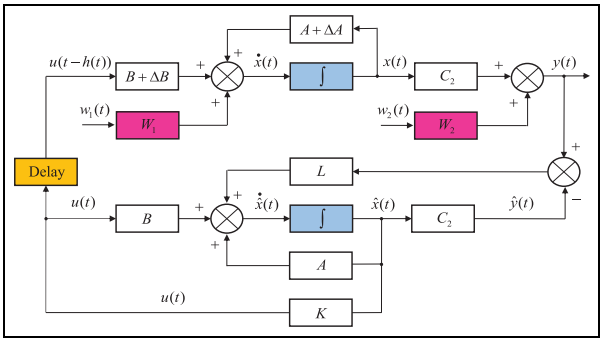

Figure 2. Block diagram of quarter-vehicle ASS.

$$\Delta A = 0.01 \times H \times \begin{bmatrix} \sin(t) & 0 & 0 & 0 \\ 0 & \sin(t) & 0 & 0 \\ 0 & 0 & \sin(t) & 0 \\ 0 & 0 & 0 & \sin(t) \end{bmatrix} \times E_1$$

$$\Delta B = 0.01 \times H \times \begin{bmatrix} \sin(t) & 0 & 0 & 0 \\ 0 & \sin(t) & 0 & 0 \\ 0 & 0 & \sin(t) & 0 \\ 0 & 0 & 0 & \sin(t) \end{bmatrix} \times E_2 \tag{42}$$

in which $E_1 = \mathrm{I}_4$, $E_2 = 0.25 \times [1;1;1;1]$, and $H = 0.20 \times \mathrm{I}_4$.

Numerical simulation without disturbances

Without regard for disturbances, the original values of system state vector and the simulation time are taken as $[-0.03; -0.012675; 0; 0]$ and 20 s respectively, then the system control output vector and the system control input signal may be obtained easily. The signal curves of acceleration of vehicle body vibration, velocity of vehicle body vibration, relative displacement of vehicle body, and relative displacement of vehicle wheel are shown as Figure 5, and the signal curve of control input with a time-varying delay is shown as Figure 6.

As shown in Figure 5, the acceleration of vehicle body vibration, the velocity of vehicle body vibration, the relative displacement of vehicle body, and the relative displacement of vehicle wheel of ASS with actuator delay and uncertainty of model parameters are convergent and asymptotically stable, and the required suspension performances can be satisfied by the designed observer-based controller. Meanwhile, as shown in Figure 6, the actuator delay of ASS is about 0.5 s, the maximum input force of this system is about 60 N, the input force tends to zero after 8 s, and the change curve of input signal can meet the system demands.

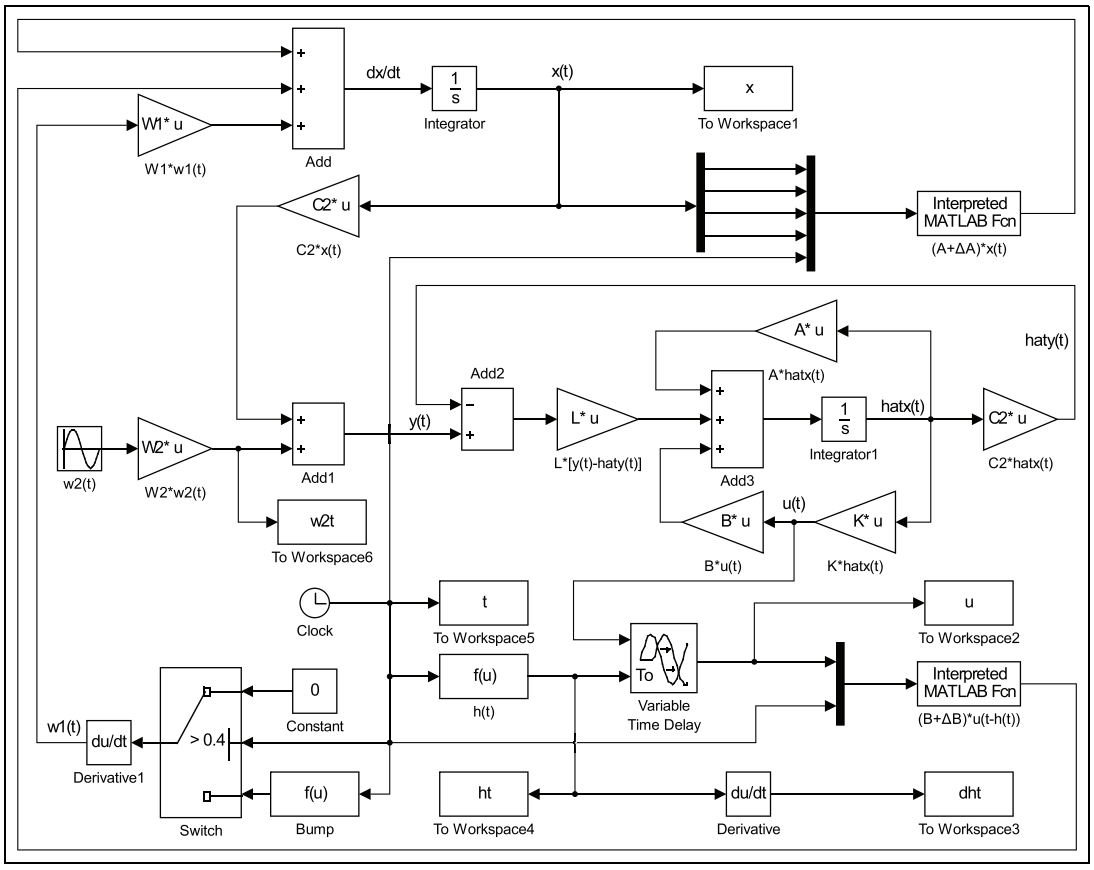

Figure 3. Numerical simulation model of dynamic output-feedback $\mathcal{H}_\infty$ control system.

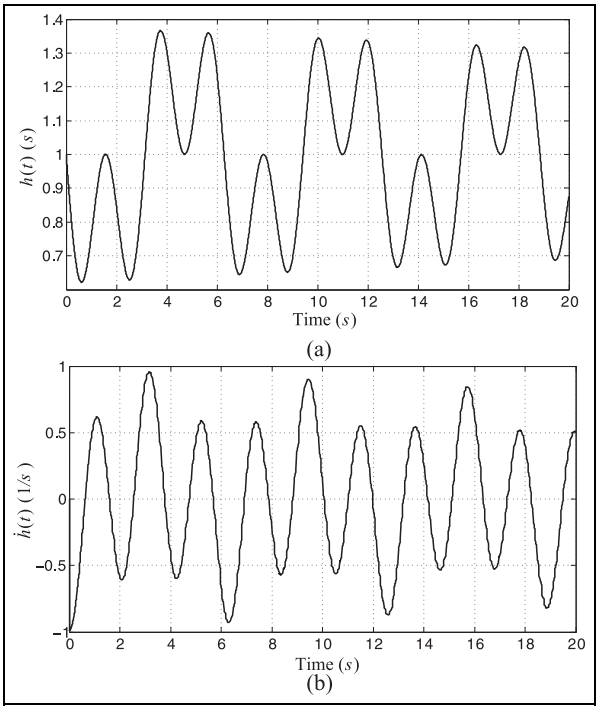

Figure 4. Time-varying input delay of actuators: (a) signal curve of $h(t)$ and (b) signal curve of $\dot{h}(t)$.

Numerical simulation with input disturbance

An isolated bump is used to demonstrate the response performances of the ASS with the proposed observer-based controller under the input disturbance caused by uneven pavement. The isolated bump is taken into account as follows[10]

$$z_r(t) = \begin{cases} \frac{H}{2}\left(1-\cos\left(\frac{2\pi v}{L}\right)t\right), & \text{when} \quad 0 \leqslant t \leqslant \frac{L}{v} \\ 0, & \text{when} \quad t > \frac{L}{v} \end{cases} \tag{43}$$

in which L and H express the length and height of the isolated bump respectively and v is the vehicle speed. Assume $L = 5$ m, $H = 0.1$ m, and $v = 12.5$ m/s, so the curve of road disturbance is expressed in Figure 7.

Without regard for output disturbance caused by sensor measurement in Figure 3, the original values of system state vector and the simulation time are taken as $[0; 0; 0; 0]$ and 20 s respectively, then the control output vector of system and the control input signal of system may be obtained easily. Meanwhile, the variation curves of main performance parameters of corresponding PSS can be achieved without consideration of system control input and time-varying delay in Figure 3. The comparison curves of acceleration of vehicle body vibration, velocity of vehicle body vibration, relative

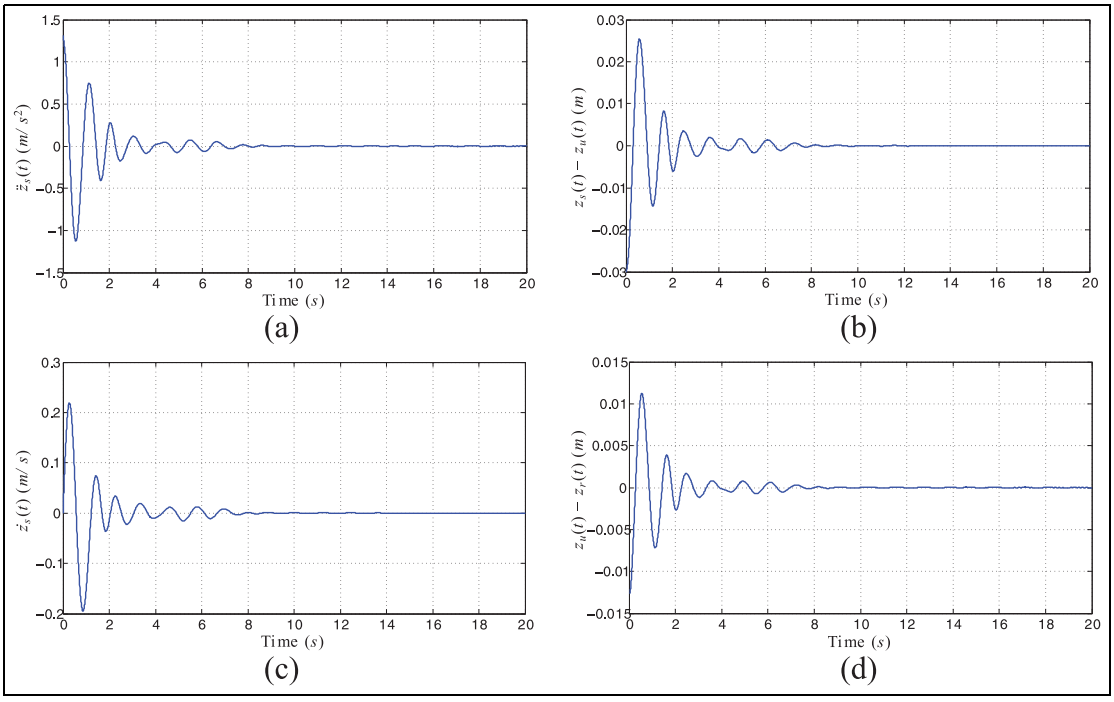

Figure 5. Signal curves of main performance parameters: (a) acceleration of vehicle body vibration, (b) velocity of vehicle body vibration, (c) relative displacement of vehicle body, and (d) relative displacement of vehicle wheel.

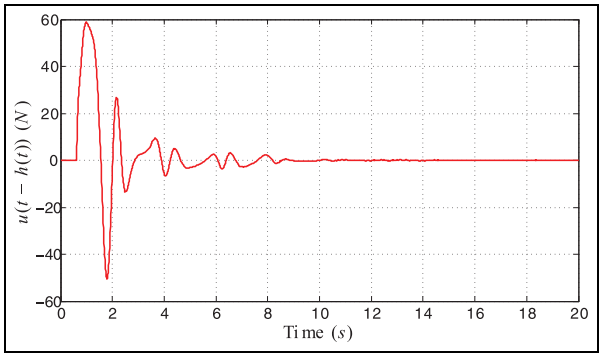

Figure 6. Signal curve of control input with a time-varying delay.

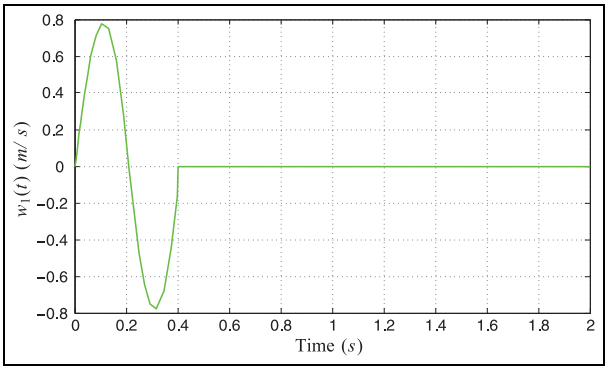

Figure 7. Input disturbance of uneven road surface.

displacement of vehicle body, and relative displacement of vehicle wheel between ASS and PSS are shown as Figure 8, and at this time, the signal curve of control input with a time-varying delay is shown as Figure 9.

As shown in Figure 8, it's easy to see that the attenuation speeds of the acceleration of vehicle body vibration, the velocity of vehicle body vibration, the relative displacement of vehicle body, and the relative displacement of vehicle wheel of ASS are all rapid relative to PSS. This indicates that the ASS using the proposed observer-based controller has better responsiveness to the input disturbance caused by the uneven road, and the better suspension performances can be satisfied by the designed observer-based controller. Meanwhile, it's easy to see from Figure 9 that the input delay of actuator is about 0.5 s, the maximum input force of this system is about 100 N, the input force tends to zero after 10 s, and the change curve of input signal can meet the system demands.

Numerical simulation with input and output disturbances

The input and output disturbances of this system are taken into account simultaneously. The input disturbance curve of uneven road surface is also shown in

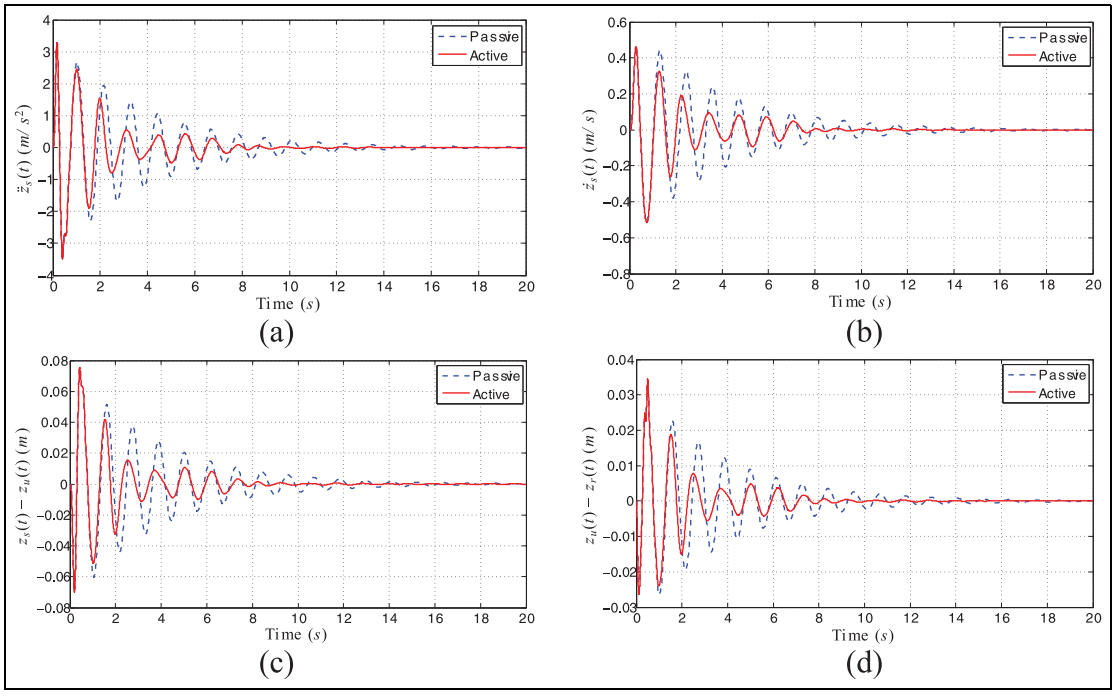

Figure 8. Comparison curves of main performance parameters: (a) acceleration of vehicle body vibration, (b) velocity of vehicle body vibration, (c) relative displacement of vehicle body, and (d) relative displacement of vehicle wheel.

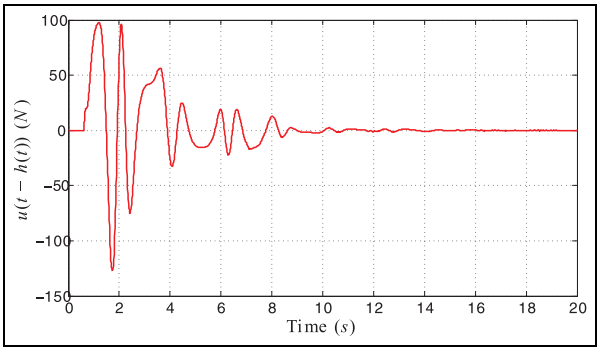

Figure 9. Signal curve of system control input for an isolated bump.

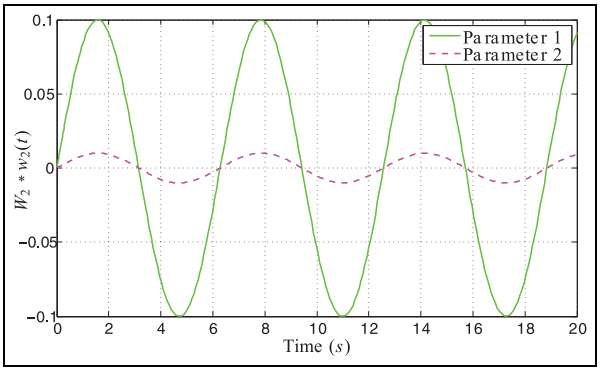

Figure 10. Output disturbance curves of sensor measurement.

Figure 7; the output disturbance caused by sensor measurement is set as $w_2(t) = \sin(t)/10$, and its gain matrix is taken as $W_2 = [1; (1/10)]$. So, the curves of output disturbance caused by sensor measurement are shown in Figure 10.

Through numerical simulation, the comparison curves of acceleration of vehicle body vibration, velocity of vehicle body vibration, relative displacement of vehicle body, and relative displacement of vehicle wheel between the ASS only with input disturbance caused by the uneven road and the ASS with both input disturbance caused by the uneven road and the output disturbance caused by sensor measurement are shown as Figure 11, and the comparison curves of system control input with a time-varying delay are shown as Figure 12.

As shown in Figure 11, it's easy to see that the two comparison curves of acceleration of vehicle body vibration, velocity of vehicle body vibration, relative displacement of vehicle body, and relative displacement of vehicle wheel respectively are almost identical. Meanwhile, it can be seen from Figure 12 that the two comparison curves of system control inputs are roughly consistent. Both of them have an actuator input delay of about 0.5 s, and both the maximum input forces of them are about 100 N. The input force of the ASS only with the input disturbance caused by the uneven road tends to zero after 10 s; nevertheless, the input force of the ASS with both the input disturbance caused by the

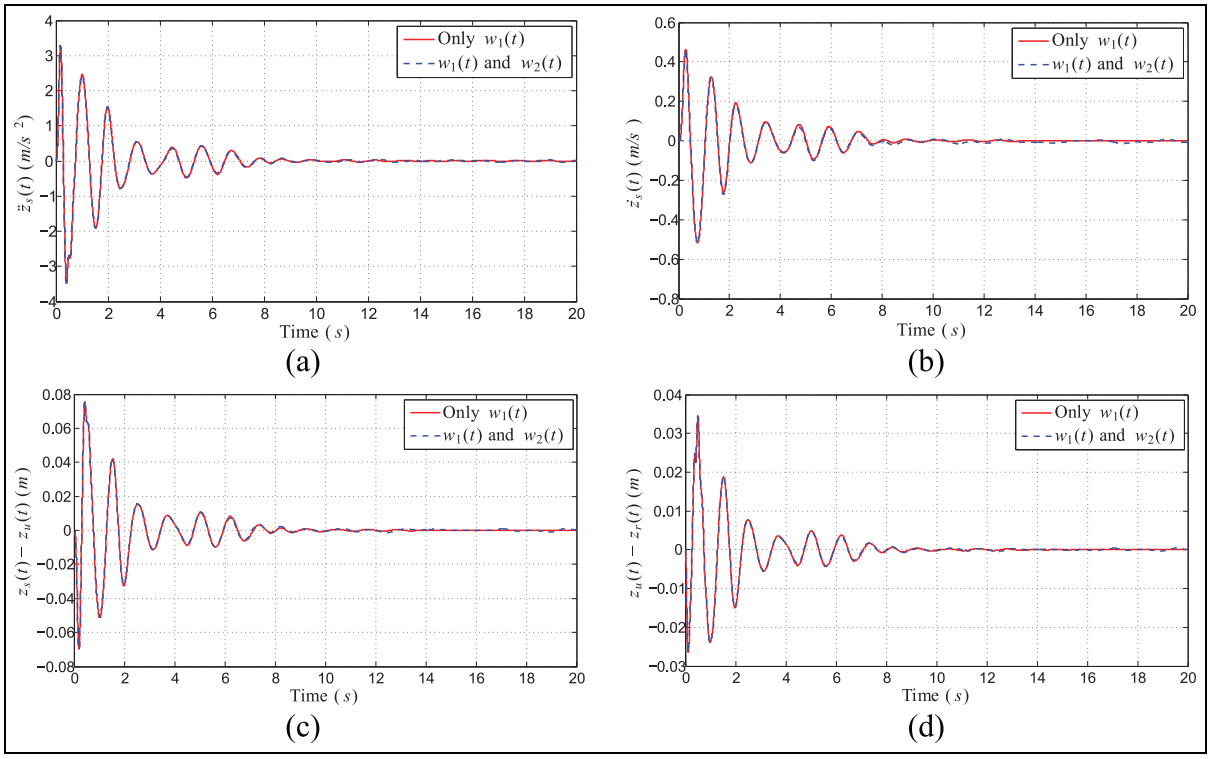

Figure 11. Comparison curves of suspension performance parameters: (a) acceleration of vehicle body vibration, (b) velocity of vehicle body vibration, (c) relative displacement of vehicle body, and (d) relative displacement of vehicle wheel.

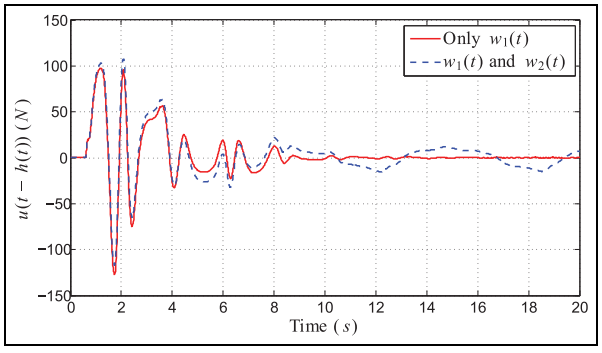

Figure 12. Comparison curves of system control inputs.

uneven road and the output disturbance caused by sensor measurement is still slightly adjusted according to the input and output disturbances after 10 s. These indicate that the developed observer-based controller for ASS can solve the problems caused by the output disturbance of sensor measurement well.

Conclusion

This article proposed a design methodology of observer-based $\mathcal{H}_\infty$ controller for quarter-vehicle ASS with input delay of actuators, uncertainty of model parameters, and input and output disturbances. First, the simplified two-degree-of-freedom model of ASS with input delay and the dynamic differential equations of this system were established, and the state equations, state observer, and observer-based controller were given separately. Second, an observer-based $\mathcal{H}_\infty$ controller for ASS was designed based on the Lyapunov–Krasovskii functional and LMIs, and the design of observer-based controller was converted into the solving problem of LMIs. Finally, the observer gain matrix and the controller gain matrix were solved by means of the designed observer-based controller and the technical parameters of selected vehicle, and three numerical simulation cases were given to verify the feasibility of the proposed scheme. The simulation results show that the designed observer-based $\mathcal{H}_\infty$ controller for quarter-vehicle ASS has good control ability and effect on time-varying input delay of actuators, uncertainty of model parameters, and input and output disturbances. In the future work, the implementation of the proposed design methodology and the observer-based adaptive fault-tolerant tracking control of ASS will be the focus of follow-up investigation.

Declaration of conflicting interests

The author(s) declared no potential conflicts of interest with respect to the research, authorship, and/or publication of this article.

Funding

The author(s) disclosed receipt of the following financial support for the research, authorship, and/or publication of this article: This work was jointly supported by the National Natural Science Foundation of China (Grants 11705122, 51705221, 51875258, and 61902268); Overseas Training Program for Universities of Jiangsu Province; Department of Building and Real Estate of the Hong Kong Polytechnic University; General Research Fund titled "Proactive Monitoring of Work-Related MSD Risk Factors and Fall Risks of Construction Workers Using Wearable Insoles" under Grant BRE/PolyU 152099/18E; General Research Fund titled "In Search of a Suitable Tool for Proactive Physical Fatigue Assessment: An Invasive to Non-Invasive Approach" under Grant PolyU 15204719/18E; Natural Science Foundation of the Hong Kong Polytechnic University (Grant G-YW3X); Research Foundation of Department of Education of Sichuan Province under Grants 17ZA0271 and 18ZA0357; Sichuan Science and Technology Program of China under Grants 19ZDZX0037, 2019YFSY0045, 2018 JY0197, and 2016SZ0074; Sichuan Key Provincial Research Base of Intelligent Tourism under Grant ZHZJ18-01; Open Foundation of Artificial Intelligence Key Laboratory of Sichuan Province under Grants 2018RZJ01 and 2017RZJ02; and Natural Science Foundation of Sichuan University of Science and Engineering under Grants 2017RCL52, 2018 RCL18, and 2017RCL12, and Zigong Science and Technology Program of China under Grants 2019YYJC03, and 2019YYJC15).

ORCID iD

Ping He https://orcid.org/0000-0001-7340-9606

References

1. Shi W and Yao W. *Automobile structure*. 6th ed. Beijing, China: China Communications Press, 2013.
2. Feng C, Lu Z and He D. *Automotive electronic control technology*. 2nd ed. Beijing, China: China Communications Press, 2011.
3. Zhao Y, Wu Q, Li H, et al. Optimization of thermal efficiency and unburned carbon in fly ash of coal-fired utility boiler via grey wolf optimizer algorithm. *IEEE Access* 2019; 7: 114414–114425.
4. Fan T, Tuo X, Li H, et al. Chaos control and circuit implementation of a class of double-wing chaotic system. *Int J Numer Model El* 2019; 32: e2611.
5. Lin Y, Chen X and Tang L. *New technology of vehicle suspension system*. Beijing, China: Beijing Institute of Technology Press, 2017.
6. He P and Fan T. Distributed fault-tolerance consensus filtering in wireless sensor networks-part I: communication failure. *Int J Sens Netw* 2016; 22: 127–142.
7. Yue YG and He P. A comprehensive survey on the reliability of mobile wireless sensor networks: taxonomy, challenges, and future directions. *Inform Fusion* 2018; 44: 188–204.
8. He P, Wang XL and Li Y. Guaranteed cost synchronization of complex networks with uncertainties and time-varying delays. *Complexity* 2016; 21: 381–395.
9. He P and Li Y. H^{∞} synchronization of coupled reaction-diffusion neural networks with mixed delays. *Complexity* 2016; 21: 42–53.
10. Li H, Jing X and Karimi HR. Output-feedback-based H_{∞} control for vehicle suspension systems with control delay. *IEEE T Ind Electron* 2014; 61: 436–446.
11. Li R, Jiao X and Yang C. Output feedback-based robust control for a half-car hydraulic active suspension system. *J Vib Shock* 2014; 33: 187–193.
12. He P. Pinning control and adaptive control for synchronization of linearly coupled reaction-diffusion neural networks with mixed delays. *Int J Adapt Control* 2018; 32: 1103–1123.
13. Choi HD, Ahn CK, Lim MT, et al. Dynamic output-feedback H^{∞} control for active half-vehicle suspension systems with time-varying input delay. *Int J Control Autom* 2016; 14: 59–68.
14. Rath JJ, Defoort M, Karimi HR, et al. Output feedback active suspension control with higher order terminal sliding mode. *IEEE T Ind Electron* 2017; 64: 1392–1403.
15. Yan G, Fang M and Xu J. Analysis and experiment of time-delayed optimal control for vehicle suspension system. *J Sound Vib* 2019; 446: 144–158.
16. Chen C, Wang G and Yu S. Preview control of vehicle active suspensions with time-varying input delay and frequency band constraints. *J Mech Eng* 2016; 52: 124–131.
17. Pedro JO, Dangor M, Dahunsi OA, et al. Dynamic neural network-based feedback linearization control of full-car suspensions using PSO. *Appl Soft Comput* 2018; 70: 723–736.
18. Badri P, Amini A and Sojoodi M. Robust fixed-order dynamic output feedback controller design for nonlinear uncertain suspension system. *Mech Syst Signal Pr* 2016; 80: 137–151.
19. Liu J, Gao Y, Su X, et al. Disturbance-observer-based control for air management of PEM fuel cell systems via sliding mode technique. *IEEE T Contr Syst T* 2019; 27: 1129–1138.
20. Wu C, Liu J, Xiong Y, et al. Observer-based adaptive fault-tolerant tracking control of nonlinear nonstrict-feedback systems. *IEEE T Neur Net Lear* 2018; 29: 3022–3033.
21. Chen H and Jiang B. A review of fault detection and diagnosis for the traction system in high-speed trains. *IEEE T Contr Syst T*. Epub ahead of print 27 February 2019. DOI: 10.1109/TITS.2019.2897583.
22. He P, Ma SH and Fan T. Finite-time mixed outer synchronization of complex networks with coupling time-varying delay. *Chaos* 2012; 22: 043151.
23. Zhao YP, He P, Saberi Nik H, et al. Robust adaptive synchronization of uncertain complex networks with multiple time-varying coupled delays. *Complexity* 2015; 20: 62–73.
24. He P, Jing CG, Fan T, et al. Robust decentralized adaptive synchronization of general complex networks with coupling delayed and uncertainties. *Complexity* 2014; 19: 10–26.

25. He P, Li Y and Park JH. Noise tolerance leader-following of high-order nonlinear dynamical multi-agent systems with switching topology and communication delay. *J Frankl Inst* 2016; 353: 108–143.
26. Wang K, He P, Tang J, et al. Static output feedback H_∞ control for active suspension system with input delay and parameter uncertainty. *Adv Mech Eng* 2018; 10: 1687814018786581.
27. He P. *Robust synchronization of dynamical networks with delay and uncertainty: synthesis & application*. PhD Thesis, Universidade de Macau, Taipa, 2017.

Appendix 1

Lemma 1

Assuming that a matrix E satisfies $E^TE \leqslant I$, then for any $x, y \in \mathbb{R}^n$, the following inequality is satisfied[27]

$$\pm 2x^TEy \leqslant x^Tx + y^Ty$$

Lemma 2

For any $x, y \in \mathbb{R}^n$, the following inequality is satisfied[27]

$$\pm 2x^Ty \leqslant x^Tx + y^Ty$$

Lemma 3

Assuming that a constant symmetric matrix $E = E^T = \begin{bmatrix} E_{11} & E_{12} \\ E_{12}^T & E_{22} \end{bmatrix}$, the following conditions are equal[27]

- $E < 0$;
- $E_{11} < 0, E_{22} - E_{12}^T E_{11}^{-1} E_{12} < 0$;
- $E_{22} < 0, E_{11} - E_{12} E_{22}^{-1} E_{12}^T < 0$.